

## Research Article

<https://doi.org/10.1631/jzus.A2200437>



# Optimal slag content for geopolymer composites under freeze-thaw cycles with different freezing temperatures

Lifeng FAN, Weiliang ZHONG, Guang WANG, Yan XI<sup>✉</sup>

*Faculty of Architecture, Civil and Transportation Engineering, Beijing University of Technology, Beijing 100124, China*

**Abstract:** Improving the freeze-thaw resistance of geopolymers is of great significance to ensure their durability in cold regions. This study presents an experimental investigation of optimal slag content for geopolymer composites under freeze-thaw cycles with different freezing temperatures. Firstly, five kinds of geopolymer composites with 10.0%, 20.0%, 30.0%, 40.0%, and 50.0% slag contents and 1.0% fiber content were prepared. Freeze-thaw cycle tests at  $-1.0\text{ }^{\circ}\text{C}$ ,  $-20.0\text{ }^{\circ}\text{C}$ , and  $-40.0\text{ }^{\circ}\text{C}$  were carried out for these geopolymer composites and their physical and mechanical properties after the freeze-thaw cycle were tested. The results show that the porosity of the geopolymer composites decreases as the slag content increases. Their mass loss ratio and strength loss ratio increase gradually as the freezing temperature decreases. The mass loss ratio and strength loss ratio of geopolymer composites after freeze-thaw cycles all decrease as the slag content increases. Considering the physical and mechanical properties of geopolymers after freeze-thaw cycles, the optimal slag contents are 40.0% and 50.0%.

**Key words:** Geopolymer composites; Freeze-thaw cycle; Freezing temperature; Slag content

## 1 Introduction

Geopolymer is an ideal cement substitute material with lower  $\text{CO}_2$  emissions and energy consumption, due to lower calcination temperature in the manufacturing process (Nasvi et al., 2013). Geopolymer can reduce  $\text{CO}_2$  emission by 80.0% compared to Portland cement in the manufacturing process (Duxson et al., 2007a, 2007b). In addition, it also exhibits excellent mechanical properties and durability, which promote its potential use in many areas, especially in some harsh environments (Richardson et al., 2016; Xie et al., 2019; Tian et al., 2021). However, freeze-thaw cycles can cause deterioration of its mechanical properties and affect the service life of constructions (Zhao RD et al., 2019; Zhang et al., 2021). The freeze-thaw resistance of geopolymer in cold environments is one of the important indexes for evaluating its practicability

and durability (Zhao MX et al., 2019; Rashad and Sadek, 2020; Yuan et al., 2020). Therefore, improving the freeze-thaw durability of geopolymer is of great significance for its wide application in severely cold areas.

The freeze-thaw resistance of cement-based materials in cold environments has been widely investigated. Generally, cement-based materials contain many capillaries, voids, bubbles, and even defects of different sizes. Under freeze-thaw cycles, the volume expansion stress on the microscopic pore structure due to the phase transition of pore water induces the micro-crack and affects the mechanical properties. Many scholars have prepared anti-freeze cement-based materials (Jacobsen et al., 1997; Chen et al., 2014; Şahin Y et al., 2021), and further studied the effect of the number of freeze-thaw cycles (Gencel et al., 2021) and the freeze-thaw method (Du et al., 2022) on the mechanical properties of such materials. However, due to the different hydration mechanisms between geopolymer and cement, the compositions and pore characteristics of geopolymer and cement are different (Parbhoo and Nagy, 1988; Fan et al., 2022). The differences in hydration products can lead to dissimilar freeze-thaw resistance in geopolymer and cement

✉ Yan XI, [xiyan@bjut.edu.cn](mailto:xiyan@bjut.edu.cn)

 Lifeng FAN, <https://orcid.org/0000-0002-7744-692X>  
Yan XI, <https://orcid.org/0000-0002-1829-6554>

Received Sept. 8, 2022; Revision accepted Jan. 21, 2023;  
Crosschecked Mar. 10, 2023

© Zhejiang University Press 2023

(Yang et al., 2020; Zhang P et al., 2020). In addition, the freeze-thaw resistance of geopolymer is still unclear due to its limited infrastructure applications. Therefore, in order to ensure the durability of geopolymer in cold environments, it is important to further study its freeze-thaw resistance.

Currently, research on the freeze-thaw resistance of metakaolin-based geopolymer materials has been carried out. Many scholars further improve the freeze-thaw resistance of geopolymer by incorporating admixtures, such as slag, silica fume, and rubber powder (Luukkonen et al., 2018; Jiao et al., 2021; Şahin F et al., 2021; Zhu et al., 2021). Among those, slag is an ideal admixture that can significantly improve the compressive strength and durability of a geopolymer (Fu et al., 2011; Shahrajabian and Behfarnia, 2018). Previous studies have mainly investigated the freeze-thaw resistance of geopolymer through freeze-thaw cycle experiments in the lab with the freezing temperature during freeze-thaw cycle experiments set to  $-20.0\text{ }^{\circ}\text{C}$  according to ASTM C666 (ASTM, 2008) or GB/T 50082-2009 (MOHURD, 2009). In that case, the slag-modified geopolymer was proven to have excellent freeze-thaw resistance. However, with the increase of building in cold regions, the ambient temperature of buildings can be lower and can even reach  $-40.0\text{ }^{\circ}\text{C}$ . Geopolymer may thus be subjected to freeze-thaw cycles with different freezing temperatures and these cause more serious freeze-thaw damage. The freeze-thaw resistance of geopolymer at different freezing temperatures is still unclear and the optimal slag content which satisfies the requirements of practical application in cold regions needs further study.

This paper mainly focuses on investigating the effect of freezing temperature on the physical and mechanical properties of slag-modified metakaolin-based geopolymer and then proposes the optimal slag content to satisfy the requirements of the practical application in cold regions. The pore structure of geopolymer with different slag contents was analyzed. The physical and mechanical properties of geopolymer after freeze-thaw cycles with different freezing temperatures were further analyzed. Finally, the optimal slag content which satisfies the requirements of practical application in cold regions is proposed. The studies are expected to provide a reference for the practical application and durability evaluation of geopolymer in cold regions.

## 2 Experimental and methods

### 2.1 Materials

The main raw materials used in this study include metakaolin, slag, water, polyvinyl alcohol (PVA) fiber, sodium hydroxide pellets, and sodium silicate. Metakaolin used in this study was provided by the Jiayu Mining Plant in Hebei Province, China. The average particle size of metakaolin is  $13.0\text{ }\mu\text{m}$ . The slag used in this study is ground granulated blast furnace slag with a specific gravity of  $2.84\text{ g/cm}^3$  and an average particle size of  $15.0\text{ }\mu\text{m}$ , which is conformed to ASTM C618 (ASTM, 2013b). Table 1 shows the chemical composition of metakaolin and slag based on the X-ray fluorescence (XRF) test. As shown in Table 1, the main chemical composition of metakaolin is  $\text{Al}_2\text{O}_3$  and  $\text{SiO}_2$ . The percentages of  $\text{Al}_2\text{O}_3$  and  $\text{SiO}_2$  are 43.99% and 48.25%, respectively. The metakaolin shows a low CaO content, only 0.70%. In addition, the main chemical components of ground granulated blast furnace slag (GGBFS) used in this study are CaO,  $\text{SiO}_2$ , and  $\text{Al}_2\text{O}_3$ , at 38.53%, 30.67%, and 15.90%, respectively. The alkaline activator was obtained by mixing sodium hydroxide, sodium silicate solution, and tap water. In this study, the purity of sodium hydroxide is 99.0% and the modulus ratio of sodium silicate solution is 3.24. The PVA fiber was produced by Kuraray Company, Japan. The length and diameter of the fiber are 12 mm and  $39.0\text{ }\mu\text{m}$ , respectively. The density of the fiber is  $1.3\text{ g/cm}^3$ . In addition, the tensile strength and elastic modulus are 1600 MPa and 42.8 GPa, respectively. The elongation of the fiber is 6.0%.

**Table 1 Chemical composition of metakaolin and slag**

Composition	Mass fraction (%)	
	Metakaolin	Slag
CaO	0.70	38.53
$\text{SiO}_2$	48.25	30.67
$\text{Al}_2\text{O}_3$	43.99	15.90
$\text{Fe}_2\text{O}_3$	3.32	0.24
$\text{TiO}_2$	2.35	1.50
MgO	0.00	8.94
Others	1.39	4.22

### 2.2 Preparation of the specimens

The mix proportions used in this experiment are shown in Table 2. As shown in Table 2, the mass replacement of metakaolin by slag was set as 10.0%, 20.0%, 30.0%, 40.0%, and 50.0%. Meanwhile, 1.0%

PVA fibers by volume were added to enhance the tensile properties of the geopolymer. The raw materials and preparation process of the geopolymer composites used in this study are shown in Fig. S1 of the electronic supplementary materials (ESM). The specific preparation method of geopolymer composites is referred to our previous study (Zhong et al., 2022b). Cube and cylindrical specimens were prepared in this study. The dimensions of the cube specimens used in physical and mechanical tests are 70.7 mm×70.7 mm×70.7 mm. The low-field nuclear magnetic resonance (LF-NMR) test was performed on cylindrical specimens with a diameter of 50.0 mm and a height of 25.0 mm.

**Table 2** Mix design proportions for the geopolymer specimens

Mix No.	Mass fraction of binder (%)		Mass ratio of activator to binder	Volume fraction of PVA fiber (%)
	Metakaolin	Slag		
S-10	90	10	0.5	1
S-20	80	20	0.5	1
S-30	70	30	0.5	1
S-40	60	40	0.5	1
S-50	50	50	0.5	1

## 2.3 Methods

### 2.3.1 Low-field nuclear magnetic resonance test

LF-NMR has been widely used in the measurement of microscopic pore structure due to its nondestructive and quantitative characteristics (Zhang A et al., 2020). In this study, the cylindrical specimens were vacuumed at  $-0.1$  MPa for 24 h and then soaked in distilled water until LF-NMR test was performed. The Macro-MR12-060H-I (Niumag Corporation, Suzhou, China) was used (Fig. S2 of ESM). The resonance frequency is 12.0 MHz and the probe coil diameter is 60.0 mm. In addition, the temperature was set to  $(32.00\pm 0.02)$  °C. The pore structure of the specimens was further investigated according to the Carr-Purcell-Meiboom-Gill (CPMG) method (Liu et al., 2021).

### 2.3.2 Freeze-thaw cycles test

Fig. 1 shows the geopolymer specimens with different slag contents used in freeze-thaw cycle tests. As shown in Fig. 1, 100 geopolymer specimens were divided into five series. The mass replacements of metakaolin by slag were 10.0%, 20.0%, 30.0%, 40.0%,

and 50.0% in series 1, 2, 3, 4, and 5, respectively. Meanwhile, each series included three different freezing temperatures, which are  $-1.0$  °C,  $-20.0$  °C, and  $-40.0$  °C. Five specimens were prepared for each freezing temperature to ensure repeatability. In addition, five geopolymer specimens cured at 20 °C were used as the control group.

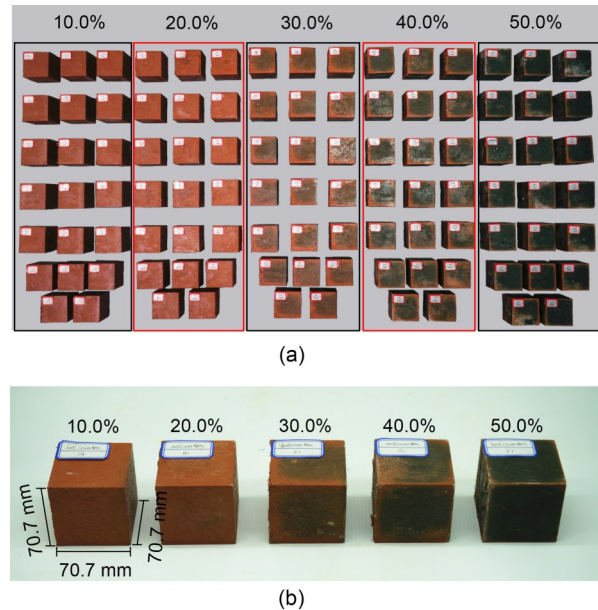


**Fig. 1** Geopolymer specimens with different slag contents used in this study: (a) geopolymer specimens used in freeze-thaw cycle tests; (b) dimension of geopolymer with different slag contents

According to GB/T 50082-2009, all geopolymer specimens were treated with vacuum saturated distilled water for 24.0 h before the freeze-thaw cycle test. During the freeze-thaw cycle treatment, each cycle contains two steps, a freezing step and a thawing step. In the freezing step, the specimens were frozen at different freezing temperatures for 2.0 h respectively. Then, in the thawing step, geopolymer specimens were uniformly immersed in water at room temperature  $(20.0\pm 0.2)$  °C for 1 h. The number of the freeze-thaw cycles was 10 and each freeze-thaw cycle lasted about 3.0 h.

### 2.3.3 Physical and mechanical property tests

To evaluate the freeze-thaw resistance of geopolymer specimens with different slag contents, the mass loss ratio, compressive strength loss ratio, and elastic modulus loss ratio were determined. After 10 freeze-thaw cycles, the mass of the geopolymer

specimens was tested. The mass loss ratio was calculated by

$$R_m = \left| \frac{M_T - M_0}{M_0} \right| \times 100\%, \quad (1)$$

where  $R_m$  is the mass loss ratio, and  $M_0$  and  $M_T$  are the masses of specimens before and after the freeze-thaw cycles, respectively. Then, a quasi-static compression test was conducted on the specimens by an electro-hydraulic servo universal testing machine with loading rate of 0.5 MPa/s (Fig. S3). The displacement was obtained using two dial indicators (ASTM, 2013a). The compressive strength loss ratio was calculated by

$$R_c = \left| \frac{\sigma_T - \sigma_0}{\sigma_0} \right| \times 100\%, \quad (2)$$

where  $R_c$  is the compressive strength loss ratio, and  $\sigma_0$  and  $\sigma_T$  are the compressive strengths of specimens before and after the freeze-thaw cycles, respectively. The elastic modulus loss ratio was calculated by

$$R_e = \left| \frac{E_T - E_0}{E_0} \right| \times 100\%, \quad (3)$$

where  $R_e$  is the elastic modulus loss ratio, and  $E_0$  and  $E_T$  are the elastic moduli of specimens before and after the freeze-thaw cycles, respectively.

### 3 Results and discussion

#### 3.1 Pore structure analysis

The phase transformation and migration of pore water in the cold environment are closely related to the pore structure of the geopolymer and affect its physical and mechanical properties after the freeze-thaw cycles. In this study, the pore structure characteristics of geopolymer composites with different slag contents were analyzed by LF-NMR. Fig. 2 shows the pore distribution of different pore sizes in geopolymer specimens with different slag contents. As shown in Fig. 2, the pore sizes ranged from  $10^{-3}$  to  $10^{-1}$   $\mu\text{m}$  show the highest proportion in geopolymer with different slag contents. In addition, the amplitude of the peaks located at  $10^{-3}$  to  $10^{-1}$   $\mu\text{m}$  decreases significantly as the slag content increases. This indicates that the incorporation of slag can reduce the number of pores ranging from  $10^{-3}$  to  $10^{-1}$   $\mu\text{m}$ . Fig. 3a shows the variation of

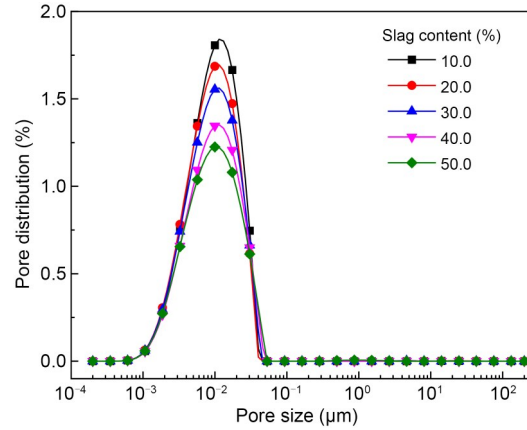


Fig. 2 Pore distribution of different pore sizes in geopolymer specimens with different slag contents

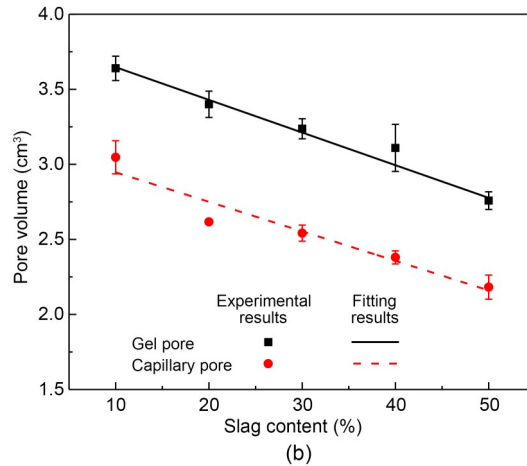
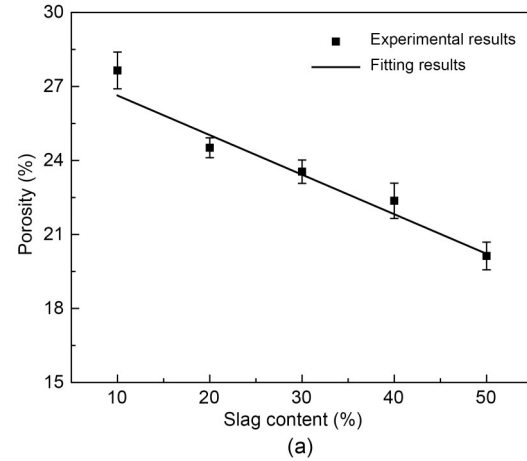


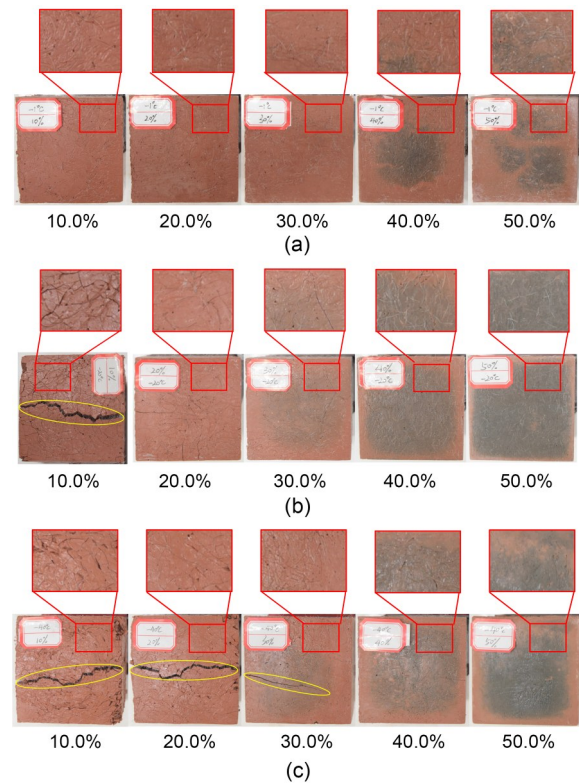
Fig. 3 Variation of the porosity of geopolymer composites with increasing slag content (a); pore volume of gel pore and capillary pore in the geopolymer composites (b)

the porosity of geopolymer composites as the slag content increases. As shown in Fig. 3a, the porosity of geopolymer composites with 10.0% slag content is

27.65%. The porosity of the geopolymer composites decreases as the slag content increases. When the slag content is 50.0%, the porosity of the geopolymer decreases to 20.13%, indicating that the geopolymer composites are densified after adding slag. In addition, the pores are divided into gel pores ( $<10$  nm) and capillary pores (10 nm–500  $\mu$ m) according to pore sizes (El-Hassan and Ismail, 2018; Zhong et al., 2022a). Fig. 3b is the effect of slag contents on the pore volume of gel pore and capillary pore in the geopolymer specimens. As shown in Fig. 3b, the gel pore volume in geopolymer composites with different slag contents is always larger than the capillary pore volume. In addition, the gel pore and capillary pore volume all decrease as the slag content increases. The variation of the pore structure of geopolymer with different slag contents can affect the freeze-thaw resistance. Thus, the variation in physical and mechanical properties of the geopolymer with different slag contents after freeze-thaw cycles was further analyzed.

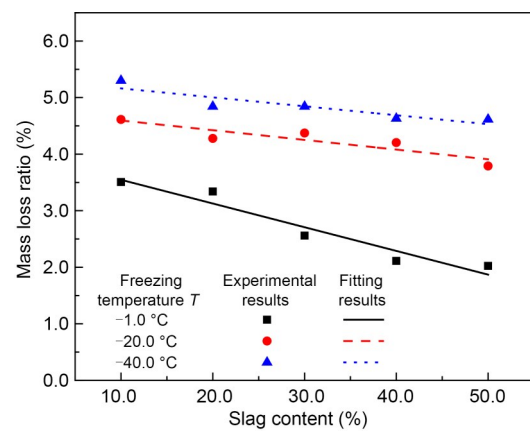
### 3.2 Variation in physical properties after freeze-thaw cycles

Fig. 4 shows the geopolymer specimens with different slag contents after freeze-thaw cycles with different freezing temperatures. As shown in Fig. 4, after 10 freeze-thaw cycles with a freezing temperature of  $-1.0$   $^{\circ}\text{C}$ , the integrity of geopolymers with different slag contents is preserved and their surfaces are flat. When the freezing temperature is  $-20.0$   $^{\circ}\text{C}$ , the integrity of a geopolymer with 10.0% slag content has been destroyed after 10 freeze-thaw cycles. A penetrating main crack can be observed on the specimen, and many micro-cracks are distributed on the specimen. Meanwhile, the main crack disappears and the number of micro-cracks on the surface of the geopolymer decreases significantly as slag content increases. When the slag contents are 40.0% and 50.0%, cracks are not observed on the surface of the geopolymer, showing that the integrity of the geopolymer specimens is preserved. When the freezing temperature is  $-40.0$   $^{\circ}\text{C}$ , the main crack and micro-cracks can be observed in the geopolymers with 10.0%, 20.0%, and 30.0% slag contents. The width of the main crack decreases and the number of micro-cracks decreases as the slag content increases. It means that the incorporation of slag can inhibit the cracking of the geopolymer and improve its freeze-thaw resistance.



**Fig. 4** Photos of geopolymer specimens with different slag contents after freeze-thaw cycles with freezing temperatures of  $-1.0$   $^{\circ}\text{C}$  (a),  $-20.0$   $^{\circ}\text{C}$  (b), and  $-40.0$   $^{\circ}\text{C}$  (c)

Fig. 5 shows the relationship between the mass loss ratio of geopolymer specimens and slag contents after freeze-thaw cycles with different freezing temperatures. The mass loss ratio can quantitatively describe the damage degree of geopolymer after the freeze-thaw cycles. As shown in Fig. 5, when the freezing temperature is  $-1.0$   $^{\circ}\text{C}$ , the mass loss ratio of



**Fig. 5** Relationship between mass loss ratio of geopolymer specimens and slag contents after freeze-thaw cycles with different freezing temperatures

all the geopolymer composites is less than 3.5%, which is consistent with a higher integrity. The mass loss ratio of geopolymer composites increases gradually as the freezing temperature decreases. Meanwhile, it also can be seen that the mass loss ratio of geopolymer composites decreases gradually as the slag content increases at the same freezing temperatures. This shows that the incorporation of slag can improve freeze-thaw resistance.

### 3.3 Deterioration analysis of mechanical properties after freeze-thaw cycles

Fig. 6 shows the quasi-static compressive stress–strain curves of geopolymer with different slag contents after freeze-thaw cycles with different freezing temperatures. As shown in Fig. 6a, the peak stress of geopolymer after curing for 28 d first increases and then decreases as the slag content increases. In addition, the slopes of the down segments of the stress–strain

curves with different slag contents are all steep, indicating that the geopolymer has better deformation resistance. As shown in Figs. 6b–6d, after freeze-thaw cycles with a freezing temperature of  $-1.0\text{ }^{\circ}\text{C}$ , the stress–strain curves of geopolymer with different slag contents change slightly. It indicates that the mechanical properties of the geopolymer are stable under freeze-thaw cycles with a freezing temperature of  $-1.0\text{ }^{\circ}\text{C}$ , which confirms the lower mass loss ratio. When the freezing temperature is  $-20.0\text{ }^{\circ}\text{C}$ , the peak stresses of geopolymers with different slag contents all decrease after the freeze-thaw cycles. Among them, the stress–strain curves of geopolymer with 10.0% and 20.0% slag contents decrease significantly. The down segments of stress–strain curves become longer and the peak strain increases significantly. This phenomenon demonstrates that the deformation resistance of geopolymer decreases significantly after freeze-thaw cycles with a freezing temperature of

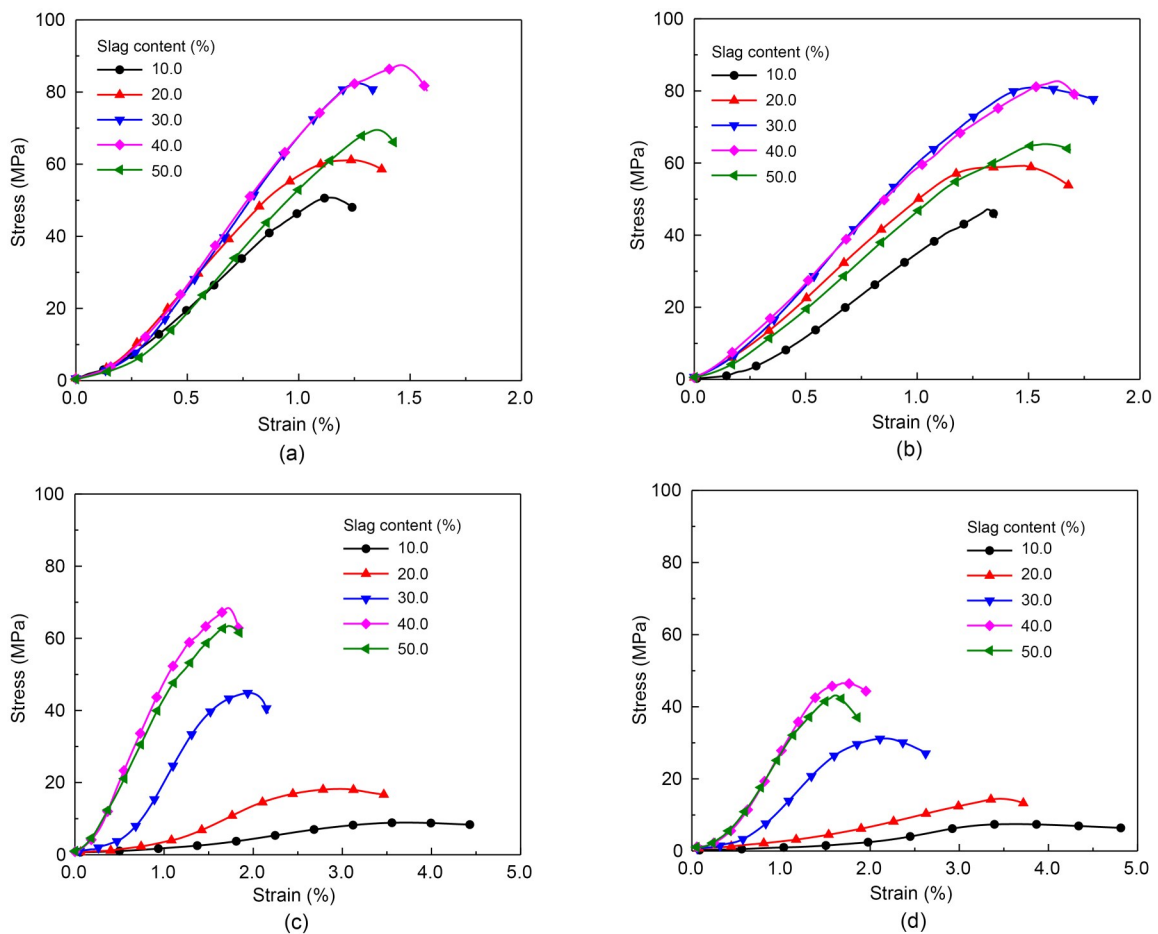
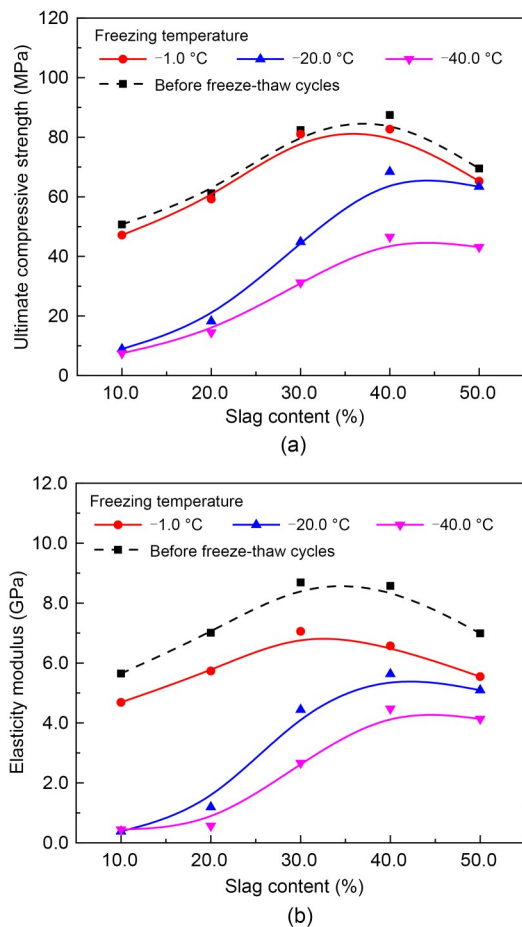


Fig. 6 Quasi-static compressive stress–strain curves of geopolymer with different slag contents after freeze-thaw cycles with different freezing temperatures: (a)  $25.0\text{ }^{\circ}\text{C}$ ; (b)  $-1.0\text{ }^{\circ}\text{C}$ ; (c)  $-20.0\text{ }^{\circ}\text{C}$ ; (d)  $-40.0\text{ }^{\circ}\text{C}$

$-20.0\text{ }^{\circ}\text{C}$ , and the failure mode gradually changes from brittleness to ductility. When the freezing temperature is  $-40.0\text{ }^{\circ}\text{C}$ , the peak stress of geopolymer with different slag contents continues to decrease after the freeze-thaw cycles.

Figs. 7a and 7b further show the relationship between ultimate compressive strength and elasticity modulus of geopolymer composites and slag contents after freeze-thaw cycles with different freezing temperatures. The elastic modulus is calculated from the elastic rising slope of the stress-strain curve. As shown in Fig. 7a, the ultimate compressive strength of geopolymer composites after curing for 28 d firstly increases and then decreases as the slag content increases. The geopolymer with 40.0% slag content exhibits the highest compressive strength, reaching 87.5 MPa. This indicates that the incorporation of slag can improve the mechanical properties of geopolymer, while



**Fig. 7** Relationship between ultimate compressive strength (a) and elasticity modulus (b) of geopolymer specimens and slag contents after freeze-thaw cycles with different freezing temperatures

excessive slag content reduces the mechanical properties, which is consistent with previous study (El-Hassan and Ismail, 2018). In addition, after freeze-thaw cycles with a freezing temperature of  $-1.0\text{ }^{\circ}\text{C}$ , the ultimate compressive strengths of geopolymer with different slag contents all decrease slightly. However, when the freezing temperature is  $-20.0\text{ }^{\circ}\text{C}$ , the ultimate compressive strength of geopolymer composites with 10.0% slag content decreases from 50.7 MPa to 8.9 MPa. Meanwhile, the ultimate compressive strength of geopolymer composites increases gradually as the slag content increases. When the slag content is 50.0%, the ultimate compressive strength of geopolymer composites only decreases by 6.0 MPa, which is 63.4 MPa. As the freezing temperature continues to decrease, the ultimate compressive strengths of geopolymer composites all decrease significantly after freeze-thaw cycles with a freezing temperature of  $-40.0\text{ }^{\circ}\text{C}$ , which is consistent with the large number of cracks shown in Fig. 4. The tendency of the elasticity modulus of geopolymer after freeze-thaw cycles with different freezing temperatures is similar to that of ultimate compressive strength, which first increases and then decreases as the slag content increases. Meanwhile, under the same slag contents, the elasticity modulus of the geopolymer decreases gradually as the freezing temperature decreases.

Fig. 8a shows the effect of the freezing temperature on the strength loss ratio of geopolymers with different slag contents. As shown in Fig. 8a, the strength loss ratios of geopolymer composites with different slag contents all increase significantly as the freezing temperature decreases. After freeze-thaw cycles with a freezing temperature of  $-1.0\text{ }^{\circ}\text{C}$ , the strength loss ratios of geopolymer with different slag contents are all less than 10%. It indicates that geopolymer composites can maintain relatively stable mechanical properties at a freezing temperature of  $-1.0\text{ }^{\circ}\text{C}$ . However, when the freezing temperature is  $-20.0\text{ }^{\circ}\text{C}$ , the geopolymer composites with different slag contents all show an increasing trend, but the rate of increase differs. Among them, the geopolymer composites with 10.0% slag content show the highest strength loss ratio, which is 82.4%. The strength loss ratio of geopolymer composites at a freezing temperature of  $-20.0\text{ }^{\circ}\text{C}$  decreases gradually as the slag content increases. When the slag content is 50.0%, the strength loss ratio of geopolymer composites is relatively

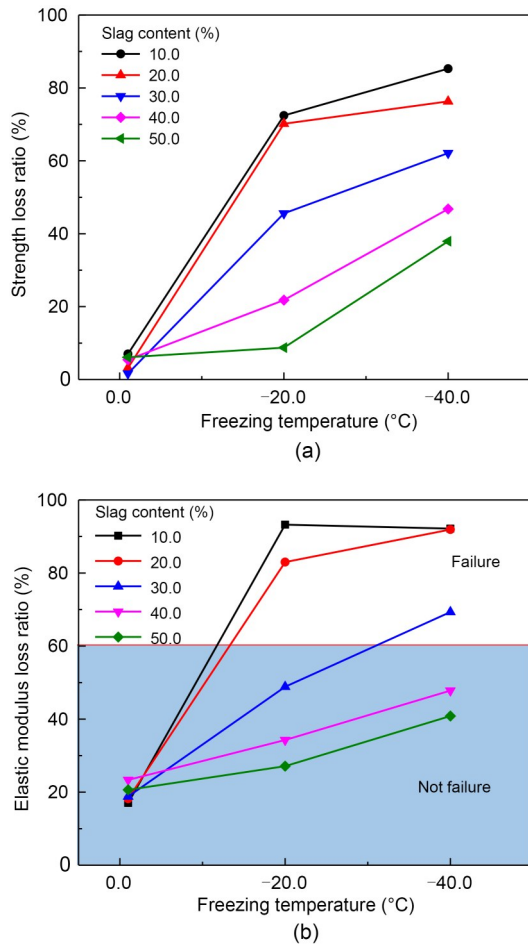


**Fig. 8** Effect of the freezing temperature on the strength loss ratio (a) and elastic modulus loss ratio (b) of geopolymer with different slag contents

stable, only increasing by 2.6%. When the freezing temperature is  $-40.0\text{ }^{\circ}\text{C}$ , the strength loss ratio of geopolymer composites with different slag contents further increases. This indicates that a decrease in freezing temperature can exacerbate freeze-thaw damage. The phenomenon can be further explained by the LF-NMR test results. The phase transformation and migration of geopolymer pore water in cold environments are closely related to the pore structure. Previous studies found that the capillary pores freeze at  $-12.0\text{ }^{\circ}\text{C}$ . Since the gel pore water molecules are attached to the solid surface, the gel pore water does not freeze above  $-78.0\text{ }^{\circ}\text{C}$  (Wang et al., 2022). As shown in Fig. 2, the pore size in the geopolymer mainly concentrates in the range of  $10^{-3}$  to  $10^{-1}\text{ }\mu\text{m}$ , which can be divided into gel pore and capillary pore. When the freezing temperature is  $-1.0\text{ }^{\circ}\text{C}$ , the water in the gel pore and capillary pore is not frozen and thus

the physical and mechanical of geopolymer composites remain stable. When the freezing temperature is  $-20.0\text{ }^{\circ}\text{C}$ , the water in the capillary pore undergoes a phase transformation as the temperature changes, causing damage to the geopolymer. Meanwhile, the capillary pore volume gradually decreases as slag content increases, resulting in the improvement of freeze-thaw resistance of geopolymer composites.

Fig. 8b shows the effect of the freezing temperature on the elastic modulus loss ratio of geopolymer with different slag contents. As shown in Fig. 8b, the variation trend of the elastic modulus loss ratio is similar to that of the strength loss ratio as the freezing temperature decreases. The elastic modulus loss ratio increases significantly as the freezing temperature decreases and decreases as the slag content increases. According to GB/T 50082-2009, the specimen is defined as in a failure state when the elastic modulus loss ratio exceeds 60.0%. As shown in Fig. 8b, when the freezing temperature is  $-1.0\text{ }^{\circ}\text{C}$ , the elastic modulus loss ratios of geopolymers with 10.0%, 20.0%, 30.0%, 40.0%, and 50.0% slag contents are all less than 60.0%. When the freezing temperature is  $-20.0\text{ }^{\circ}\text{C}$ , the elastic modulus loss ratio of geopolymer with 30.0%, 40.0%, and 50.0% slag contents is less than 60.0%. When the freezing temperature is  $-40.0\text{ }^{\circ}\text{C}$ , the elastic modulus loss ratio of geopolymer with 40.0% and 50.0% slag contents is less than 60.0%. To determine the optimal slag contents, Fig. 9 further shows a comprehensive analysis of the compressive strength and elastic modulus of the geopolymer composites after freeze-thaw cycles with different freezing temperatures. As shown in Fig. 9, the geopolymer composites with 40.0% and 50.0% slag contents still preserve high mechanical properties after freeze-thaw cycles with different freezing temperatures, which are all larger than

Freezing temperature ( $^{\circ}\text{C}$ )	Slag content (%)				
	10.0	20.0	30.0	40.0	50.0
-1.0	47.15 (4.69)	59.23 (5.73)	81.05 (7.06)	82.71 (6.57)	65.25 (5.55)
-20.0	8.91 (0.38)	18.24 (1.19)	44.85 (4.44)	68.40 (5.63)	63.42 (5.10)
-40.0	7.46 (0.44)	14.48 (0.57)	31.20 (2.67)	46.54 (4.48)	43.14 (4.13)

■ Suggested slag content

**Fig. 9** Comprehensive analysis of compressive strength and elastic modulus of the geopolymer composites after freeze-thaw cycles with different freezing temperatures. The values in each cell refer to  $\sigma(E)$ , where  $\sigma$  is the compressive strength (MPa), and  $E$  is the elastic modulus (GPa)

40.0 MPa. It indicates that the geopolymer composites with 40.0% and 50.0% slag contents can be used as a cementitious material to replace PO 42.5 cement and have potential application prospects in severe cold areas. In addition, the compressive strength and elastic modulus of geopolymer after freeze-thaw cycles with different freezing temperatures can also be observed in Fig. 9, which can provide a reference for the application of geopolymers in practical engineering.

This paper mainly focuses on investigating the effect of freezing temperature on the physical and mechanical properties of slag-modified metakaolin-based geopolymers and proposes the slag content to satisfy the requirement of practical application in cold regions. The theoretical research of the freeze-thaw mechanism of geopolymer is also in the framework of an overall project and will be further investigated. In addition, the slag-modified metakaolin-based geopolymer in this study is a cementitious material, which can provide a reference for further research on the freeze-thaw resistance of geopolymer mortar and concrete.

## 4 Conclusions

This study presents an experimental investigation of optimal slag content for the geopolymer composites under freeze-thaw cycles with different freezing temperatures. The following conclusions can be drawn:

1. The porosity of geopolymer composites decreases as slag content increases, indicating that the incorporation of slag content can significantly compact the geopolymer composites. Meanwhile, the gel pore and transition pore volume proportions all decrease as the slag content increases.

2. The freeze-thaw damage of geopolymer composites is more serious as the freezing temperature decreases, but the damage degree of the geopolymer composites decreases as slag content increases. The width and number of cracks in geopolymer composites after freeze-thaw cycles all decrease as the slag content increases, indicating that the incorporation of slag can inhibit the cracking of the geopolymer in cold environments.

3. The incorporation of the slag can significantly reduce the mass loss ratio and strength loss ratio of geopolymer composites after freeze-thaw cycles and

improve the freeze-thaw resistance of geopolymer composites.

4. The geopolymer composites with 40.0% and 50.0% slag contents still preserve high mechanical properties after freeze-thaw cycles with different freezing temperatures and have potential application prospects in cold areas.

## Acknowledgments

This work is supported by the National Natural Science Foundation of China (No. 51627812).

## Author contributions

Lifeng FAN designed the research. Lifeng FAN and Yan XI processed the corresponding data. Guang WANG wrote the first draft of the manuscript. Guang WANG and Weiliang ZHONG helped to organize the manuscript. Lifeng FAN and Weiliang ZHONG revised and edited the final version.

## Conflict of interest

Lifeng FAN, Weiliang ZHONG, Guang WANG, and Yan XI declare that they have no conflict of interest.

## References

- ASTM (American Society for Testing and Materials), 2008. Standard Test Method for Resistance of Concrete to Rapid Freezing and Thawing, ASTM C666. ASTM.
- ASTM (American Society for Testing and Materials), 2013a. Standard Test Method for Compressive Strength of Hydraulic Cement Mortars (Using 2-in. or [50-mm] Cube Specimens), ASTM C109. ASTM.
- ASTM (American Society for Testing and Materials), 2013b. Standard Specification for Coal Fly Ash and Raw of Calcined Natural Pozzolan for Use in Concrete, ASTM C618. ASTM.
- Chen CH, Zhu PH, Wu JY, et al., 2014. Research on frost resistance of recycled high performance concrete. *Applied Mechanics and Materials*, 584-586:1456-1460. <https://doi.org/10.4028/www.scientific.net/AMM.584-586.1456>
- Du T, Zhou B, Liu B, et al., 2022. The influence of opposite-side high temperature on the frozen behavior of containment concrete under single-side salt freeze-thaw method. *Structures*, 36:854-863. <https://doi.org/10.1016/j.istruc.2021.12.063>
- Duxson P, Fernández-Jiménez A, Provis JL, et al., 2007a. Geopolymer technology: the current state of the art. *Journal of Materials Science*, 42(9):2917-2933. <https://doi.org/10.1007/s10853-006-0637-z>
- Duxson P, Provis JL, Lukey GC, et al., 2007b. The role of inorganic polymer technology in the development of 'green concrete'. *Cement and Concrete Research*, 37(12):1590-1597. <https://doi.org/10.1016/j.cemconres.2007.08.018>

- El-Hassan H, Ismail N, 2018. Effect of process parameters on the performance of fly ash/GGBS blended geopolymer composites. *Journal of Sustainable Cement-Based Materials*, 7(2):122-140.  
<https://doi.org/10.1080/21650373.2017.1411296>
- Fan LF, Zhong WL, Zhang YH, 2022. Effect of the composition and concentration of geopolymer pore solution on the passivation characteristics of reinforcement. *Construction and Building Materials*, 319:126128.  
<https://doi.org/10.1016/j.conbuildmat.2021.126128>
- Fu YW, Cai LC, Cai YG, 2011. Freeze-thaw cycle test and damage mechanics models of alkali-activated slag concrete. *Construction and Building Materials*, 25(7):3144-3148.  
<https://doi.org/10.1016/j.conbuildmat.2010.12.006>
- Gencel O, Benli A, Bayraktar OY, et al., 2021. Effect of waste marble powder and rice husk ash on the microstructural, physico-mechanical and transport properties of foam concretes exposed to high temperatures and freeze-thaw cycles. *Construction and Building Materials*, 291:123374.  
<https://doi.org/10.1016/j.conbuildmat.2021.123374>
- Jacobsen S, Soether DH, Sellevold EJ, 1997. Frost testing of high strength concrete: frost/salt scaling at different cooling rates. *Materials and Structures*, 30(1):33-42.  
<https://doi.org/10.1007/BF02498738>
- Jiao ZZ, Li XY, Yu QL, 2021. Effect of curing conditions on freeze-thaw resistance of geopolymer mortars containing various calcium resources. *Construction and Building Materials*, 323:125507.  
<https://doi.org/10.1016/j.conbuildmat.2021.125507>
- Liu L, He Z, Cai XH, et al., 2021. Application of low-field NMR to the pore structure of concrete. *Applied Magnetic Resonance*, 52(1):15-31.  
<https://doi.org/10.1007/s00723-020-01229-7>
- Luukkonen T, Abdollahnejad Z, Yliniemi J, et al., 2018. Comparison of alkali and silica sources in one-part alkali-activated blast furnace slag mortar. *Journal of Cleaner Production*, 187:171-179.  
<https://doi.org/10.1016/j.jclepro.2018.03.202>
- MOHURD (Ministry of Housing and Urban-Rural Development), 2009. Standard for Test Methods of Long-Term Performance and Durability of Ordinary Concrete, GB/T 50082-2009. National Standards of the People's Republic of China.
- Nasvi MCM, Ranjith PG, Sanjayan J, 2013. The permeability of geopolymer at down-hole stress conditions: application for carbon dioxide sequestration wells. *Applied Energy*, 102:1391-1398.  
<https://doi.org/10.1016/j.apenergy.2012.09.004>
- Parbhoo B, Nagy O, 1988. Molecular dynamics in hydrogen bond forming environments. The role of hydrophilic-hydrophobic interactions in pyridine-water mixtures. *Journal of Molecular Structure*, 177:393-399.  
[https://doi.org/10.1016/0022-2860\(88\)80104-2](https://doi.org/10.1016/0022-2860(88)80104-2)
- Rashad AM, Sadek DM, 2020. Behavior of alkali-activated slag pastes blended with waste rubber powder under the effect of freeze/thaw cycles and severe sulfate attack. *Construction and Building Materials*, 265:120716.  
<https://doi.org/10.1016/j.conbuildmat.2020.120716>
- Richardson A, Coventry K, Edmondson V, et al., 2016. Crumb rubber used in concrete to provide freeze-thaw protection (optimal particle size). *Journal of Cleaner Production*, 112:599-606.  
<https://doi.org/10.1016/j.jclepro.2015.08.028>
- Şahin F, Uysal M, Canpolat O, et al., 2021. The effect of polyvinyl fibers on metakaolin-based geopolymer mortars with different aggregate filling. *Construction and Building Materials*, 300:124257.  
<https://doi.org/10.1016/j.conbuildmat.2021.124257>
- Şahin Y, Akkaya Y, Tasdemir MA, 2021. Effects of freezing conditions on the frost resistance and microstructure of concrete. *Construction and Building Materials*, 270:121458.  
<https://doi.org/10.1016/j.conbuildmat.2020.121458>
- Shahrajabian F, Behfarnia K, 2018. The effects of nano particles on freeze and thaw resistance of alkali-activated slag concrete. *Construction and Building Materials*, 176:172-178.  
<https://doi.org/10.1016/j.conbuildmat.2018.05.033>
- Tian LY, He DP, Zhao JN, et al., 2021. Durability of geopolymers and geopolymer concretes: a review. *Reviews on Advanced Materials Science*, 60(1):1-14.  
<https://doi.org/10.1515/rams-2021-0002>
- Wang RJ, Hu ZY, Li Y, et al., 2022. Review on the deterioration and approaches to enhance the durability of concrete in the freeze-thaw environment. *Construction and Building Materials*, 321:126371.  
<https://doi.org/10.1016/j.conbuildmat.2022.126371>
- Xie JH, Zhao JB, Wang JJ, et al., 2019. Sulfate resistance of recycled aggregate concrete with GGBS and fly ash-based geopolymer. *Materials*, 12(8):1247.  
<https://doi.org/10.3390/ma12081247>
- Yang MJ, Paudel SR, Asa E, 2020. Comparison of pore structure in alkali activated fly ash geopolymer and ordinary concrete due to alkali-silica reaction using micro-computed tomography. *Construction and Building Materials*, 236:117524.  
<https://doi.org/10.1016/j.conbuildmat.2019.117524>
- Yuan Y, Zhao RD, Li R, et al., 2020. Frost resistance of fiber-reinforced blended slag and Class F fly ash-based geopolymer concrete under the coupling effect of freeze-thaw cycling and axial compressive loading. *Construction and Building Materials*, 250:118831.  
<https://doi.org/10.1016/j.conbuildmat.2020.118831>
- Zhang A, Yang WC, Ge Y, et al., 2020. Study on the hydration and moisture transport of white cement containing nanomaterials by using low field nuclear magnetic resonance. *Construction and Building Materials*, 249:118788.  
<https://doi.org/10.1016/j.conbuildmat.2020.118788>
- Zhang BF, Feng Y, Xie JH, et al., 2021. Rubberized geopolymer concrete: dependence of mechanical properties and freeze-thaw resistance on replacement ratio of crumb rubber. *Construction and Building Materials*, 310:125248.  
<https://doi.org/10.1016/j.conbuildmat.2021.125248>
- Zhong WL, Fan LF, Zhang YH, 2022a. Experimental research on the dynamic compressive properties of lightweight slag based geopolymer. *Ceramics International*, 48:20426-20437.  
<https://doi.org/10.1016/j.ceramint.2022.03.328>
- Zhong WL, Zhang YH, Fan LF, et al., 2022b. Effect of PDMS

- content on waterproofing and mechanical properties of geopolymer composites. *Ceramics International*, 48:26248-26257.  
<https://doi.org/10.1016/j.ceramint.2022.05.306>
- Zhang P, Wang KX, Li QF, et al., 2020. Fabrication and engineering properties of concretes based on geopolymers/alkali-activated binders—a review. *Journal of Cleaner Production*, 258:120896.  
<https://doi.org/10.1016/j.jclepro.2020.120896>
- Zhao MX, Zhang GP, Htet KW, et al., 2019. Freeze-thaw durability of red mud slurry-Class F fly ash-based geopolymer: effect of curing conditions. *Construction and Building Materials*, 215:381-390.  
<https://doi.org/10.1016/j.conbuildmat.2019.04.235>
- Zhao RD, Yuan Y, Cheng ZQ, et al., 2019. Freeze-thaw resistance of Class F fly ash-based geopolymer concrete. *Construction and Building Materials*, 222:474-483.  
<https://doi.org/10.1016/j.conbuildmat.2019.06.166>
- Zhu HJ, Zhai MN, Liang GW, et al., 2021. Experimental study on the freezing resistance and microstructure of alkali-activated slag in the presence of rice husk ash. *Journal of Building Engineering*, 38:102173.  
<https://doi.org/10.1016/j.jobbe.2021.102173>

### **Electronic supplementary materials**

Figs. S1–S3